Theoret. Chim. Acta (Berl.) 67, 413–424 (1984)

THEORETICA CHIMICA ACTA


# An application of the virial theorem to study $AH_2$ structures II. Use of CNDO/2 wavefunctions

**Rogério Custodio and Yuji Takahata**

Instituto de Química, Universidade Estadual de Campinas, Caixa Postal, 6154, 13.100 Campinas, São Paulo, Brazil

The simple form for the virial theorem for polyatomic molecules takes the form $W = -\Sigma t_i$ where $t_i$ is an orbital kinetic energy. It is applied to study shapes of molecules of $AH_2$ type. Kinetic-energy-*versus*-angle diagrams are constructed with CNDO/2 wavefunctions that satisfy the virial theorem. The shapes of the molecules can be explained with the aid of the diagrams.

**Key words:** Virial theorem—$AH_2$ geometry—kinetic energy—CNDO/2—correlation diagrams

## 1. Introduction

The simple form for the virial theorem for polyatomic molecules was given by Nelander [1]. It has been applied for molecules of type $AH_2$ by Takahata and Parr (henceforth referred to as I) [2]. The simple form for the virial theorem takes the form that the relation $W = -T$ holds between the total energy $W$ and the total kinetic energy $T$ not only at the equilibrium geometry of a polyatomic molecule, but also for bond angle distorted from equilibrium, if the bond distances are optimized for each set of angles. An immediate consequence is that the total energy can be expressed as a sum of negative orbital kinetic energies within the Hartree-Fock scheme:

$$W = \Sigma_i(-t_i). \tag{1}$$

It was pointed out that Eq. (1) makes it possible to partition the total energy, $W$, (including nuclear-nuclear repulsion) into genuinely additive one-electron components, $t_i$. Negative-kinetic-energies-*versus*-angle diagrams for $H_2O$, $CH_2$ and $BeH_2$ were presented in I. Principal results obtained in I were: (1) the

diagrams differs from a conventional Walsh diagram, (2) the kinetic energy diagram varies from one molecule to another. The kinetic energy diagrams were applied to explain molecular shapes. Although it was possible to explain some structural aspects of the molecules with the diagrams, it was far from complete. There still remain various aspects to be investigated as to applicability of the virial theorem to polyatomic molecules.

Löwdin states, "the fulfilment of the virial theorem is a *necessary* but *not sufficient* criterion that a wave function is an accurate solution of the Schrödinger equation corresponding to a stationary state" [3]. Therefore one cannot expect to apply the virial theorem to improve the quality of the wavefunction. However, it provides a mathematical method that can be useful in analysing and understanding the nature of a molecule. Our object is to explore this possibility extending the previous work done in part I.

The CNDO/2 method is used to calculate wavefunctions of $AH_2$ type molecules. In order to satisfy the polyatomic virial theorem, the bond distances have to be optimized at each set of angles. This is a time-consuming procedure if *ab initio* calculations are to be applied. It is our interest to study whether the virial theorem can be usefully applied with CNDO/2 wavefunctions. If its results are affirmative, we can apply the theorem to more complicated polyatomic molecules than $AH_2$ without much computational burden. The CNDO/2 wavefunctions have to be scaled in order to satisfy the virial theorem. Löwdin showed how to calculate the scaling factor and the scaled wavefunctions for a diatomic molecule [3]. He also stated that the method developed for the diatomic molecule could be directly generalizable to a polyatomic system. A generalization to a polyatomic system was made [4] and applied to the $AH_2$ type molecules in I. The same procedure is applied here to the $AH_2^Q$ type molecules where $Q$ is the charge taking the value of 0 (zero) or $\pm 1$, and $A$ = F, O, N, C, B and Be. CNDO/2 orbital kinetic energies are calculated using the formula given by Roothan [5].

## 2. Results and discussion

Table 1 shows equilibrium bond angles and bond lengths ($R_{eq}$), scaling factors ($\eta_{eq}$) at the equilibrium structures calculated with CNDO/2 wavefunctions. The calculated bond lengths are in good agreement with experimental values. The calculated bond angles agree reasonably well with observed ones. Agreement between theory and experiment is better for the bond lengths than for bond angles. The scaling factors ($\eta_{eq}$) varies from a molecule to another.

Before we analyze the behavior of molecular orbital kinetic energies of the molecules of the $AH_2$ type, it is instructive to study the behavior of kinetic energies of atomic orbitals of the central heavy atoms $A$ in the molecules. Fig. 1 shows a plot of the kinetic energies of $2s$ and $2p$ as a function of atomic number of $A$. It increases as the atomic number increases. This is a consequence of contraction of $2p$ and $2s$ orbitals with increase of atomic number. The kinetic energy of an electron increases as it is confined in smaller space due to the contraction.

**Table 1.** Equilibrium structures and scaling factors ($\eta_{eq}$) calculated with application of the virial theorem using CNDO/2 wavefunctions

| Number of valence electrons | Mol. | Angle calc. | Angle expt. | $R_{eq.}$ calc. | $R_{eq.}$ expt. | $\eta_{eq.}$ | Ref. |
|---|---|---|---|---|---|---|---|
| 8 | $FH_2^+$ | 85.4 | 118.1 | 0.945 | 0.920 | 1.194 | 6 |
| | $H_2O$ | 92.0 | 104.5 | 0.984 | 0.980 | 1.146 | 7 |
| | $NH_2^-$ | 98.5 | 104.0 | 1.104 | 1.066 | 1.098 | 6, 7 |
| 7 | $H_2O^+$ | 89.9 | 110.0 | 0.968 | 0.960 | 1.182 | 8, 9 |
| | $NH_2$ | 94.7 | 103.3 | 1.009 | 1.020 | 1.168 | 7, 10 |
| | $CH_2^-$ | 102.9 | 99.0 | 1.142 | 1.144 | 1.058 | 11, 12 |
| 6 | $NH_2^+$ | 90.8 | 115.0 | 0.997 | 1.038 | 1.259 | 12, 13 |
| | $CH_2$ trip. | 129.8 | 136.0 | 1.076 | 1.040 | 1.137 | 14a |
| | $CH_2$ sing. | 98.2 | 103.2 | 0.998 | 1.120 | 1.168 | 14a |
| | $BH_2^-$ | 108.1 | 102.0 | 1.241 | 1.275 | 1.008 | 12, 15 |
| 5 | $CH_2^+$ | 131.6 | 136.9 | 1.034 | 1.093 | 1.292 | 12 |
| | $BH_2$ | 133.3 | 131.0 | 1.149 | 1.180 | 1.092 | 14b |
| | $BeH_2^-$ | 128.4 | — | 1.427 | — | 1.039 | — |
| 4 | $BH_2^+$ | 180.0 | 180.0 | 1.089 | 1.140 | 1.205 | 14b |
| | $BeH_2$ | 180.0 | 180.0 | 1.308 | 1.343 | 1.024 | 14b |

It is noteworthy that the difference of the kinetic energies of $2s$ and $2p$ increases also as atomic number increases. The rate of increase of $2p$ kinetic energy is greater than that of $2s$.

Figure 2 shows a plot of orbital kinetic energy ($t_i$) of $H_2O$ molecule as a function of bond angle. If this diagram is compared with the original Walsh diagram of $AH_2$ system [16], general appearance is strikingly similar. The relative order of the orbital kinetic energy, $1b_1 > 3a_1 > 1b_2 > 2a_1$, is the same as those in the Walsh diagram. The general trend of the change of each curve is similar in the two diagrams. Only exception is $1b_1$ which decreases in Fig. 2 whereas it remains constant in the Walsh diagram. Qualitative explanation of the relative order and behavior of the individual orbital can be found with the aid of Fig. 1. The kinetic energy of $2p$ is substantially greater than that of $2s$ and $1s_H$ orbital of hydrogen atom. The $1b_1$ molecular orbital (MO) consists of pure $2p$ orbital of oxygen. All the other molecular orbitals consist of the mixture of $2p$, $2s$ and $1s_H$. This explains why the $1b_1$ has the largest kinetic energy and is located uppermost position in Fig. 2. The order of the rest depends on the degree in which $2p$ participates for a MO. The $3a_1$ becomes pure $2p$ orbital at bond angle 180°. As the bond angle decreases, the proportion of $2s$ increases. The greater the proportion of $2s$, the smaller the value of the kinetic energy. This is why the kinetic energy of $3a_1$

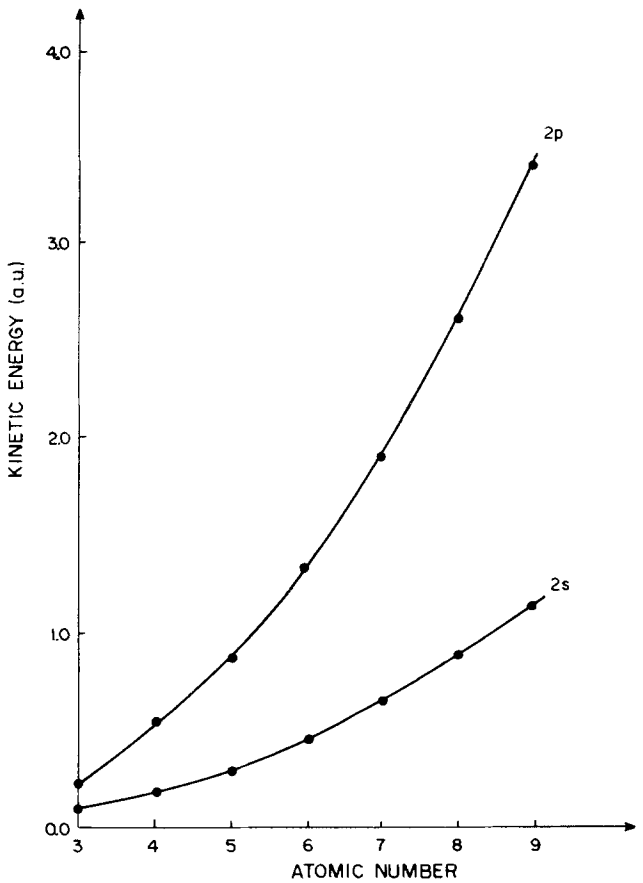


**Fig. 1.** Kinetic energies for $2s$ and $2p$ atomic orbitals for the first row elements of periodic table

decreases as the bond angle decreases. The $1b_2$ MO consists of $2p$ orbital of oxygen and $1s_H$ orbitals of hydrogen. There is substantial increase of contribution of $1s_H$ orbitals in the $1b_2$ MO as the molecule becomes linear. There is build-up of electronic charge in the $1s_H$ orbitals reducing $1b_2$ kinetic energy as the bond angle increases. The $2a_1$ MO mainly consists of $2s$ orbital of oxygen which explains why the $2a_1$ has the smallest kinetic energy in the figure. All the molecules studied with 7 and 8 valence electrons showed correlation diagrams similar to Fig. 2.

Figure 3 plots orbital kinetic energies against bond angle of $BH_2$ molecule. A resides on the tendencies of the variation of $3a_1$ and $2a_1$ with change of the bond angle. The $3a_1$ energy increases with the bond angle in both Fig. 2 and Fig. 3. The behavior of $2a_1$ is just opposite to that of $3a_1$. Differences in the two figures reside on the facts that, first, the order of $1b_2$ and $3a_1$ is interchanged, second, $1b_2$ increases with the increase of bond angle in $BH_2$ whereas it decreases in $H_2O$. The behavior of individual molecular orbitals in Fig. 3 can be attributed

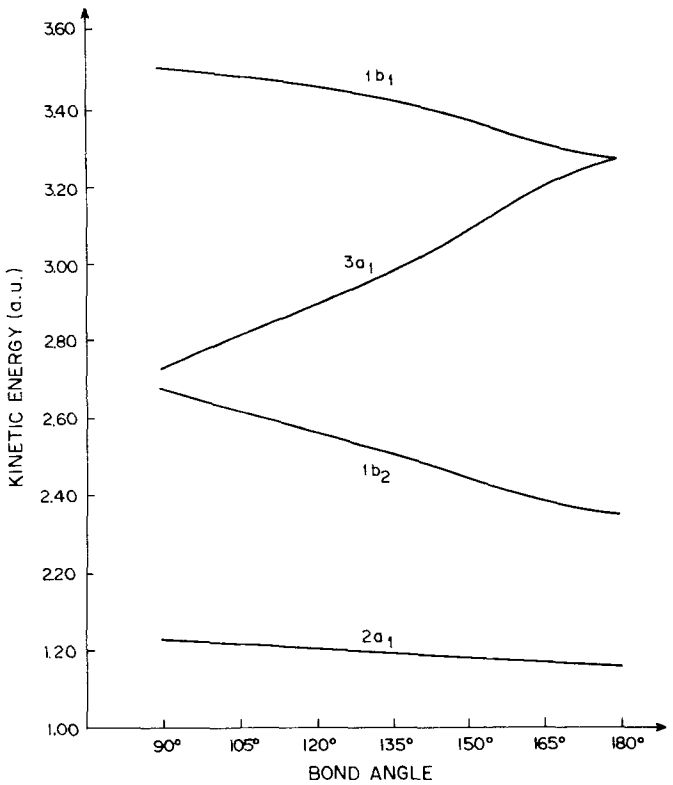


**Fig. 2.** Kinetic energy correlation diagram for $H_2O$

to a large proportion of covalent nature of B-H bond. A plot of Mulliken population analysis of $BH_2$ with respect to the bond angle shows that the overlap population between $2p$ of boron atom and $1s$ of hydrogen atom parallels to the $1b_2$ curve.

As the electronegativity of a central heavy atom $A$ becomes close to that of hydrogen atom, the influence of the hydrogen atom in chemical bond of the molecule, $AH_2$, increases. All the molecules with 5 or 4 valence electrons treated present correlation diagrams similar to Fig. 3. A correlation diagram of $BeH_2$ is similar to Fig. 3 except that there is no $3a_1$ curve because only $2a_1$ and $1b_2$ are occupied orbitals in $BeH_2$.

With this information we conclude that the kinetic diagram varies from one molecule to another. There is no universal kinetic correlation diagram. The same result is obtained in I.

The virial theorem in the form $W = -T$ indicates that the total kinetic energy takes its *maximum* value at the equilibrium geometry. Because of Eq. (1), each orbital kinetic energy must contain information about the geometry of a molecule.

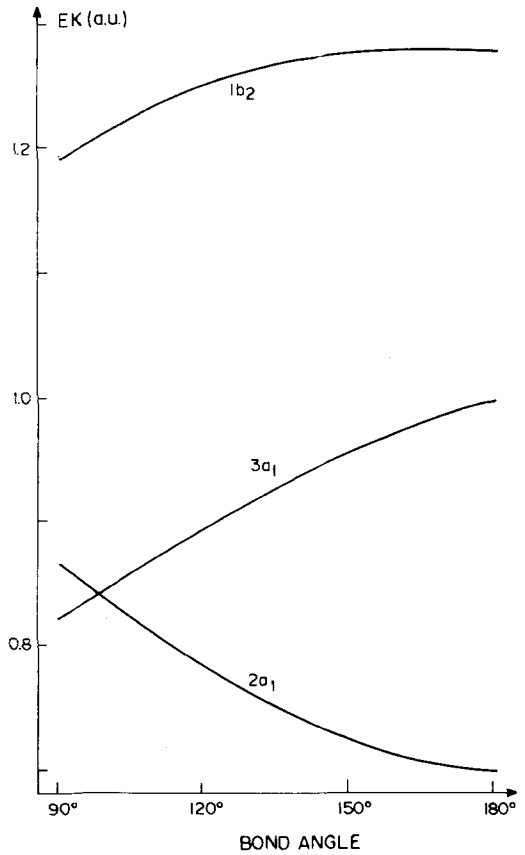


**Fig. 3.** Kinetic energy correlation diagram for $BH_2$

Therefore, the kinetic correlation diagrams such as Figs. 2 and 3 can be useful in studying molecular structure.

$BeH_2$ is linear. It has 4 valence electrons. But $BeH_2^-$ ion is bent with 5 valence electrons. Fig. 4 compares the total kinetic energies of the two molecules as a function of bond angle. The kinetic energy of $BeH_2$ shows its maximum value at 180° reflecting its linear structure. The kinetic energy of $BeH_2^-$ ion takes its maximum value at bond angle of 128° which corresponds to the equilibrium geometry of the ion. Fig. 5 plots relative quantities of orbital kinetic energies of $BeH_2$ and $BeH_2^-$. $BeH_2$ has two occupied molecular orbitals, $1b_2$ and $2a_1$. The $1b_2$ kinetic energy increases with bond angle, whereas $2a_1$ shows a trend completely opposite to $1b_2$. $BeH_2$ is linear because $1b_2$ takes its maximum value at 180°. The effect of $2a_1$ is just the opposite to that of the $1b_2$. The $2a_1$ has the tendency of reducing the bond angle. The kinetic energy of the $1b_2$ predominate that of the $2a_1$. This is the reason why the curve corresponding to the total kinetic energy of $BeH_2$ in Fig. 4 is parallel to that of the $1b_2$ in Fig. 5. It is the $1b_2$ that makes the molecule linear.

The $BeH_2^-$ ion has three occupied molecular orbitals, $2a_1$, $1b_2$ and $3a_1$. The $3a_1$

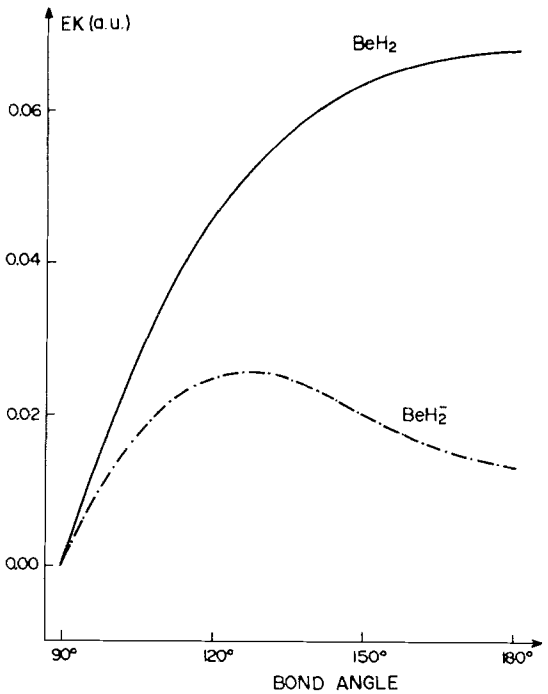


**Fig. 4.** Relative total kinetic energy diagram for $BeH_2$ and $BeH_2^-$

is singly occupied whereas the other two are doubly occupied. The bent structure of the ion is due to the presence of the $3a_1$ electron. The relative kinetic energies of the three orbitals are also included in Fig. 5. A principal effect of the presence of the $3a_1$ electron is reduction of the kinetic energy of $1b_2$ electrons, in comparison to the corresponding counterpart of $BeH_2$ molecule. The $3a_1$ electron in $BeH_2^-$ repels the $1b_2$ electrons causing expansion of the electron cloud away from the nucleus. This is why the $1b_2$ kinetic energy drops and becomes less sensitive to the geometrical change. The $2a_1$ is not much affected by the presence of the $3a_1$ electron as evidenced by a small difference between the solid and broken line of $2a_1$ in Fig. 5. The $2a_1$ causes a bent structure while both $3a_1$ and $1b_2$ cause a linear form of $BeH_2^-$. Since both theory and experiment indicate a bent structure of $BeH_2^-$, one can conclude that the reduction of $1b_2$ is the principal cause of non-linearity of the ion.

As the second example of an application of a kinetic energy diagram, $BH_2^Q$ where $Q=+1, 0, -1$, will be studied. $BH_2^+$ is linear whereas $BH_2$ and $BH_2^-$ are both bent as verified in Table 1. The number of valence electrons of $BH_2^+$, $BH_2$ and $BH_2^-$ are 4, 5, and 6 respectively. The relation between the number of valence electrons and bond angle is exactly what Walsh's rules predict [16]. $BH_2^+$ is linear because it has 4 valence electrons. $BH_2$ and $BH_2^-$ are bent because they have more than 4 valence electrons. It is of common practice to invoke the Walsh diagram [16] to explain shapes of molecules. The 5th and 6th valence electrons of $BH_2$ and $BH_2^-$ occupies $3a_1$ orbital which increases sharply with bond angle.

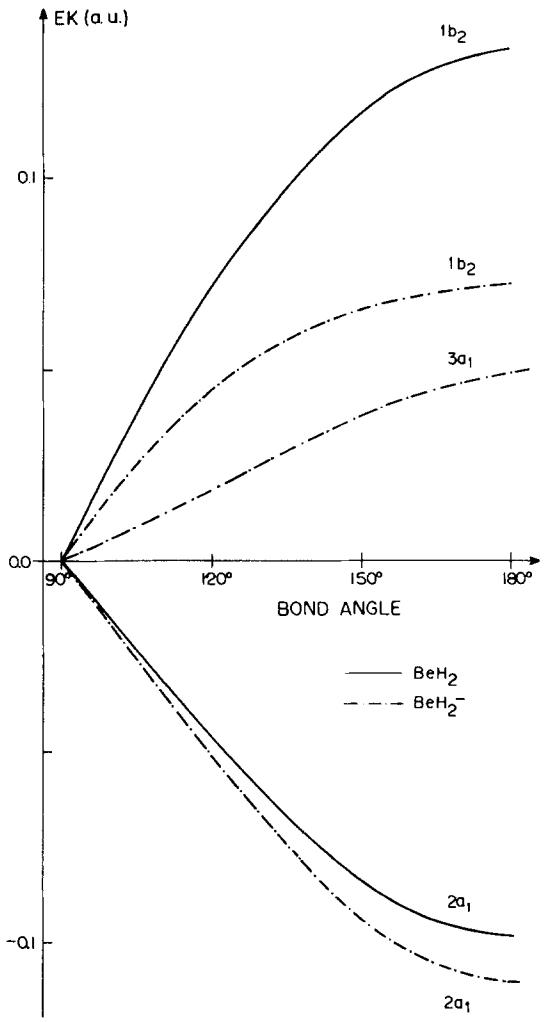


**Fig. 5.** Relative kinetic energies of molecular orbitals of $BeH_2$ and $BeH_2^-$

It is of interest to see how a kinetic energy diagram can be used to explain the differences of the shapes of the molecules. Fig. 6 presents three curves corresponding to relative total kinetic energies of $BH_2^+$, $BH_2$ and $BH_2^-$. $BH_2^+$ is linear because it has the maximum kinetic energy at 180°. The kinetic energies of $BH_2$ and $BH_2^-$ have maximum values at bond angle less than 180°.

Figure 7 compares $2a_1$ kinetic energies of the three molecules. There are no big differences between the three curves. The kinetic energy of $2a_1$ remains fairly constant with increase or decrease of $3a_1$ electrons. Figure 8 compares relative changes of $1b_2$ kinetic energies of the three molecules. $BH_2^+$ curve increases by far the most of all three showing its maximum at 180°. The rate of increase of $1b_2$ kinetic energy of $BH_2^+$ (Fig. 8) exceeds that of decrease of $2a_1$ kinetic energy (Fig. 7) resulting in the monotonic increase of the total kinetic energy with bond

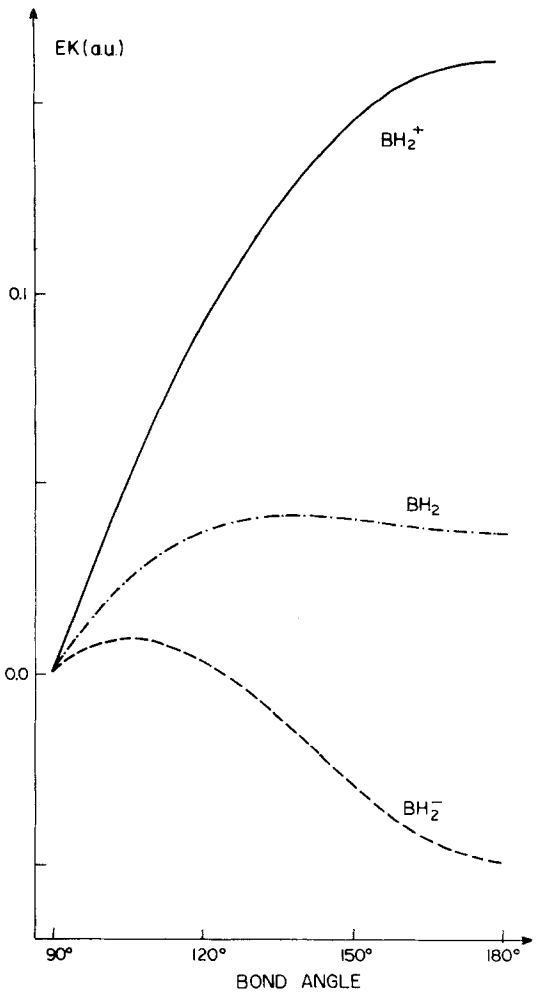


**Fig. 6.** Relative total kinetic energy diagram for $BH_2^+$, $BH_2$ and $BH_2^-$

angle (Fig. 6). Therefore, like in the case of $BeH_2$, $BH_2^+$ is linear because of the predominance of $1b_2$ kinetic energy.

In case of $BH_2$, the rate of increase of $1b_2$ kinetic energy is less than half of that of $BH_2^+$ (Fig. 8). This is a consequence of the presence of one additional electron in $3a_1$ which causes a substantial modification of the distribution of electron cloud in $1b_2$. In the region of bond angle close to 180°, $2a_1$ dominates the behavior of total kinetic energy whereas $1b_2$ and $3a_1$ dominate in the region of bond angle near 90° establishing the equilibrium angle of 133° (Exp. 131°). The similar arguments apply for $BH_2^-$ with more accentuated manner than the case of $BH_2$. The presence of 2 electrons in the $3a_1$ orbital causes expansion of $1b_2$ orbital in greater magnitude than the case of $BH_2$ reducing $1b_2$ kinetic energy further, as seen in Fig. 8. The $1b_2$ kinetic energy of $BH_2^-$ shows a maximum at bond angle around 140°. Substantial decrease of the $1b_2$ kinetic energy of $BH_2^-$ as well as

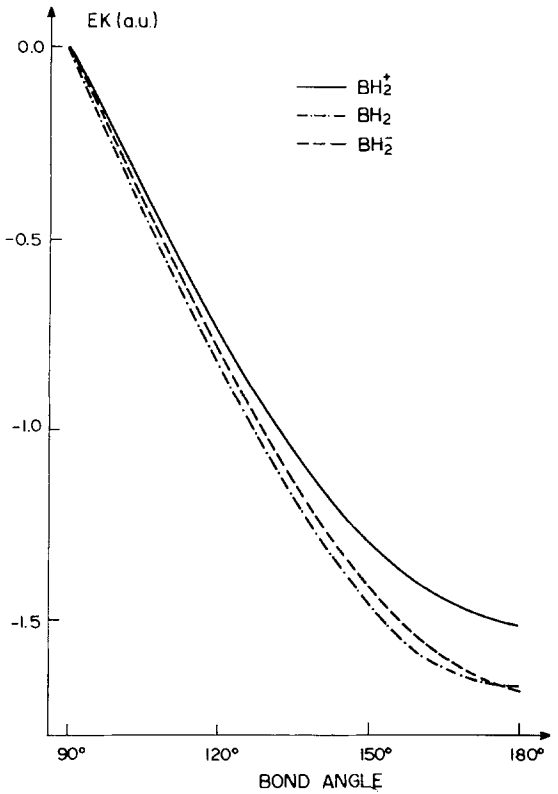


**Fig. 7.** $2a_1$ relative kinetic energies of $BH_2^+$, $BH_2$ and $BH_2^-$

the change of pattern of the curve in comparison to $BH_2$ is the principal cause of the decrease of bond angle from 133° ($BH_2$) to 108° ($BH_2^-$).

Recently Koga and Kobayashi [17] applied the virial theorem in the form of Eq. (1) to construct negative-kinetic-energy-*versus*-angle diagrams of $BH_2^-$ and $BH_2^+$ using *ab initio* wave functions. They used the GAUSSIAN 80 program package with the 6-31G** basis for the calculations. One of their conclusions is that the highest $a_1$ orbitals is important to determine the shapes of the molecules. A comparison between Koga and Kobayashi's diagrams and present CNDO/2 ones (Fig. 7 and 8) reveals some similarities and dissimilarities. The $1b_2$, for example, behaves in a similar, but $2a_1$ and $3a_1$ in a different way. Consequently, the way to explain the shapes of the molecules is somewhat different in the two methods. The CNDO/2 method is a semi-empirical model that is different from the rigorous Hartree-Fock-Roothaan method. It is, therefore, expected that CNDO/2 calculations on certain physical properties, such as kinetic energy, of a molecule do not necessarily reproduce rigorous *ab initio* calculations. However, it is of interest to make a detailed comparative study of the semi-empirical and non-empirical method in the application of the virial theorem. A work in this line has already been started in our laboratory.

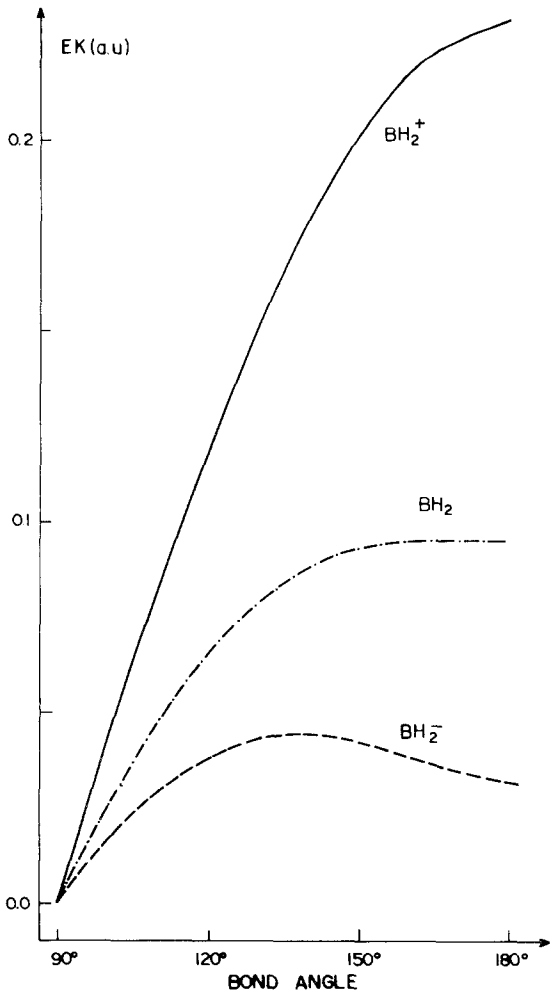


**Fig. 8.** $1b_2$ relative kinetic energies of $BH_2^+$, $BH_2$ and $BH_2^-$

When the atomic number of central atom is greater than five, the behavior of $1b_2$ starts to change. It tends to have a maximum at angle less than 180°. Another effect is that $2a_1$ orbital starts to feel the presence of $3a_1$ electrons. These happen because of the contraction of the electron cloud due to the increase of atomic number.

## 3. Conclusion

Application of the virial theorem in construction of correlation diagrams for $AH_2$ systems using CNDO/2 wavefunctions has shown that the correlation diagrams thus obtained vary from one molecule to another. There is no universal diagram such as Walsh's. Similar results are obtained in Part I where the *ab initio* method is applied.

The virial theorem indicates that molecular kinetic energy takes its maximum value at its equilibrium structure. This principle is applied to explain the molecular structure of the $AH_2$ systems. Using the correlation diagrams of orbital kinetic energies, it is possible to know which molecular orbital(s) prefer(s) a linear, which one(s) prefer(s) a bent structure. Change of molecular geometry upon increase of number of valence electron $BeH_2$ (linear) $\rightarrow$ $BeH_2^-$ (bent), for instance, is explained nicely with the aid of relative correlation diagrams of the two molecules.

The virial theorem for triatomic molecules is demonstrated to be useful as an interpretative tool which the ordinary Walsh type diagram cannot provide. It is shown that scaled CNDO/2 wavefunctions which satisfy the virial theorem can be useful in elucidating the nature of molecular geometry of a polyatomic molecule.

*Acknowledgments.* The authors wish to thank Dr. Robert G. Parr for reading an original manuscript and for kind suggestions. The authors are also indebted to CNPq and FAPESP for the scholarship and financial support. The services and computer time made available by the computer center of UNICAMP are acknowledged.

## References

1. Nelander, B.: J. Chem. Phys., **51**, 469 (1969)
2. Takahata, Y., Parr, R. G.: Bull. Chem. Soc. Japan, **47**, 1380 (1974)
3. Löwdin, P. O.: J. Mol. Spectry., **3**, 46 (1959)
4. Takahata, Y.: Ph.D. Thesis, The Johns Hopkins University, 1970
5. Roothaan, C. C.: J. Chem. Phys. **19**, 1445 (1951)
6. van Hirschausen, H., Ilten, D. F., Zeeck, E.: Chem. Phys. Lett. **40**, 80 (1976)
7. Tables of Interatomic Distances and Configurations in Molecules, Chem. Soc. Spec. Publ., no. 18 (1965)
8. Lew, H., Heiber, I.: J. Chem. Phys. **58**, 1246 (1973)
9. Sakai, H., Yamaba, S., Yamaba, T., Fukui, K.: Chem. Phys. Lett. **25**, 541 (1974)
10. Dixon, R. N.: Mol. Phys. **9**, 357 (1965)
11. Zittel, P. F., Ellison, G. B., O'Neil, S. V., Herbst, E., Lineberger, W. C., Reinhardt, W. P.: J. Am. Chem. Soc. **98**, 107 (1966)
12. Bews, J. R., Glidewell, C.: Inorg. Chim. Acta. **39**, 217 (1980)
13. Chu, S. Y., Siv, A. K. Q., Hayes, E. F.: J. Am. Chem. Soc. **94**, 2969 (1972)
14. a) Herzberg, G., Johns, K. W. C.: J. Chem. Phys. **54**, 2276 (1971); b) Herzberg, G., Johns, K. W. C.: Proc. Roy. Soc. London **A298**, 142 (1967)
15. a) Peyerinhoff, S. D., Buenker, R. J., Allen, L. C.: J. Chem. Phys. **45**, 734 (1966); b) Jungen, M.: Chem. Phys. Lett. **5**, 241 (1970)
16. Walsh, A. D.: J. Chem. Soc., 2260, 2266, 2288, 2296, 2301 (1953)
17. Koga, T., Kobayashi, H.: Theoret. Chem. Acta (Berl.) **65**, 303 (1984)

Received July 4, 1984/October 30, 1984